

Generic Contrast Agents

Our portfolio is growing to serve you better. Now you have a *choice*.



[VIEW CATALOG](#)

AJNR

Comparison of 128-Section Single-Shot Technique with Conventional Spiral Multisection CT for Imaging of the Temporal Bone

S.A. Schwab, S. Eberle, B. Adamietz, M.A. Kuefner, M. Kramer, M. Uder and M. Lell

This information is current as of May 6, 2025.

AJNR Am J Neuroradiol 2012, 33 (4) E55-E60

doi: <https://doi.org/10.3174/ajnr.A2420>

<http://www.ajnr.org/content/33/4/E55>

TECHNICAL NOTE

S.A. Schwab
S. Eberle
B. Adamietz
M.A. Kuefner
M. Kramer
M. Uder
M. Lell

Comparison of 128-Section Single-Shot Technique with Conventional Spiral Multisection CT for Imaging of the Temporal Bone

BACKGROUND AND PURPOSE: Computed tomography is an essential modality for imaging of the temporal bone. Newest generation scanners allow the coverage of large examination volumes with a single gantry rotation. The objective of this study was to compare a 128-section SST (1 single rotation of the x-ray tube) with conventional spiral MSCT (ultra-high-resolution mode) for imaging of the temporal bone.

MATERIALS AND METHODS: Fifty-four temporal bones in 27 patients were scanned with both a conventional MSCT and 128-section SST. After blinding and randomization of both examinations, 2 observers assessed the visualization of 38 anatomic structures (eg, various segments of the facial nerve canal, malleal ligaments) by using multiplanar reconstructions in the axial and coronal planes. The differences in evaluation scores obtained for the 2 techniques were analyzed by using a Wilcoxon signed rank test, with a P value of $< .05$ considered significant. For both methods, imaging time and radiation exposure were noted.

RESULTS: Overall visualization of anatomic structures did not differ significantly between the 2 techniques ($P > .05$). When we compared the anatomic structures separately, there was better visualization of the lateral malleal ligament with MSCT, whereas the cochlear septa were ranked higher with SST ($P < .05$). Imaging time and average DLP for MSCT were 12.3 seconds and 306 mGy cm, respectively; for SST, values they were 1 second and 64 mGy cm, respectively (ie, a dose reduction of 79%).

CONCLUSIONS: For imaging of the temporal bone with adequate diagnostic quality, 128-section SST can be used. The main advantages over MSCT are the dramatic reductions of imaging time and radiation exposure, which are particularly important when scanning uncooperative patients or children.

ABBREVIATIONS: CTDI_{vol} = CT dose index; DLP = dose-length product; MPR = multiplanar reformations; MSCT = multisection CT; SST = single-shot technique

CT is an essential method for imaging of the temporal bone.¹⁻⁴ Ongoing developments in CT led to a steady rise in the number of detectors (multidetector CT) and, therefore, an increase in examination volume within 1 rotation of the x-ray tube. The latest generation of scanners allows coverage of whole organs with a single gantry rotation.⁵ The major advantage is a dramatic reduction of motion artifacts and radiation exposure.

The aim of this study was to evaluate a 128-section SST, in which the whole temporal bone can be covered with a single tube rotation, and to compare this with conventional spiral MSCT in terms of image quality, examination time, and radiation exposure.

Materials and Methods

Patients

From February 2008 to March 2009, 27 patients (16 men, 11 women) referred to the department of radiology for CT of suspected inflammation or tumors of the temporal bone were included in the study

after they gave their written informed consent. Ages ranged from 33 to 84 years (mean, 51 years). Only patients not suitable for MR imaging were included. The study was conducted under an institutional review board–approved protocol.

Imaging Technique

All examinations were performed on a 128-section CT system (Somatom Definition AS+; Siemens Healthcare, Erlangen, Germany). All included patients underwent our standard unenhanced MSCT, followed by SST after intravenous injection of iodinated contrast media (Imeron 350 mg/ml; Bracco Altana Pharma, Konstanz, Germany). MSCT of the temporal bone is routinely performed in the ultra-high-resolution mode, using a special grid in front of the detector array to increase spatial resolution. The data of SST were acquired within a single rotation of the x-ray tube, by using 128 sections with a total volume coverage of 38.4 mm. Technical details for both MSCT and SST are given in Table 1.

Both imaging time and dose (DLP, CTDI_{vol}) were compared between the 2 techniques.

Image Evaluation

The examinations were reviewed on a dedicated CT workstation (syngo Multimodality Workplace, Siemens Healthcare) by using MPRs in the axial and coronal planes. Because the image thickness of MSCT was 0.4 mm and of SST was 0.75 mm, all examinations were evaluated at a constant MPR thickness of 0.8 mm; windowing was 4000 HU at a center of 700 HU. A board-certified radiologist (S.A.S.) with >5 years of experience in imaging of the temporal bone and a

From the Department of Radiology, University Hospital Erlangen-Nuremberg, Erlangen, Germany.

Paper previously presented at: Annual Meeting of the Radiological Society of North America, November 28–December 3, 2010, Chicago, Illinois; Annual Meeting of the European Congress of Radiology, March 4–8, 2010, Vienna, Austria; and Annual Meeting of the German Congress of Radiology, May 12–14, 2010, Berlin, Germany.

Please address correspondence to Siegfried A. Schwab, MD, Department of Radiology, University Hospital Erlangen-Nuremberg, Maximiliansplatz 1, D-91054 Erlangen, Germany; e-mail: siegfried.schwab@uk-erlangen.de

<http://dx.doi.org/10.3174/ajnr.A2420>

Table 1: Technical details for MSCT and SST		
Details	SST	MSCT
Tube voltage	120 kV	120 kV
Tube current	250 mAs	230 mAs
Collimated section thickness (mm)	0.75	0.4
Number of sections per rotation	128	16
Collimation (mm)	0.6	0.3
Rotation time	1	1
Pitch	— ^a	0.8
Reconstruction algorithm	B75h	U75u
FOV	200	141
Mean examination duration (seconds)	1	12.29

^a—indicates no pitch with SST.

Table 2: Evaluated anatomic structures of the temporal bone	
No.	Structure
1	Scutum
2	Anulus tympanicus
3	Tympanic membrane
4	Malleus head
5	Malleus handle
6	Incudomalleolar articulation
7	Anterior malleolar ligament
8	Lateral malleolar ligament
9	Superior malleolar ligament
10	Incus body
11	Incus long process
12	Incus short process
13	Incus lenticular process
14	Incudostapedial articulation
15	Stapes footplate
16	Stapes crura
17	Stapes capitulum
18	Facial recess
20	Sinus tympani
21	Tendon of the musculus tensor tympani
22	Cochleariform process
23	Stapedius muscle
24	Körner septum
25	Round window niche
26	Round window membrane
27	Oval window
28	Bone septum between upper and middle turn of the cochlea
29	Cochlear aqueduct
30	Vestibular aqueduct
31	Crista falciformis
32	Modiolus
33	Ampulla membranaceum
34	Facial nerve canal: labyrinthine segment
35	Facial nerve canal: geniculate ganglion
36	Facial nerve canal: tympanic segment
37	Facial nerve canal: mastoid segment
38	Bony coverage of the facial nerve in the tympanic segment

resident (S.E.) evaluated the examinations after blinding and random ordering in a consensus reading. Before the actual evaluations, both S.A.S. and S.E. trained for the assessment process by using dedicated literature about the CT anatomy of the temporal bone.⁶ The training cases were not included in the study.

For the evaluation of the CT images of the temporal bone, 38 anatomic structures were chosen (Table 2), in accordance with previously published studies.^{1,2,4,7}

The assessment of each anatomic structure was performed by using the following scale: 1 = not visible because of insufficient image quality, 2 = visible but not diagnostic, 3 = visible and diagnostic.¹

Table 3: Score scheme for the assessment of the detectability of each anatomic structure	
Score	Interpretation
1	Not visible because of image quality
2	Visible but not diagnostic
3	Visible and diagnostic
4	Not detectable due to disease or surgery

Structures that were not detectable because of disease or surgery were classified as 4 (Table 3) and were excluded from statistical analysis as “missing data.”

Statistics

The difference in the visibility of the defined anatomic structures in MSCT and SST was compared by using a Wilcoxon signed rank test; a *P* value < .05 was considered significant. A normal distribution was excluded by using the Kolmogorov-Smirnov test (*P* < .05). Bonferroni correction was applied to compensate for effects of multiple testing. All statistical analyses were performed by using dedicated software, the Statistical Package for the Social Sciences, Version 14.0 (SPSS, Chicago, Illinois).

Results

Fifty-four temporal bones from 27 patients scanned with both SST and MSCT were evaluated by the readers. Category 4 (not detectable because of disease or surgery, 3.3% of the entire dataset) was excluded from statistical analysis as missing data. No SST was degraded by motion artifacts.

Overall visualization of the 38 anatomic structures did not differ significantly between SST and MSCT (*P* < .05) (Figs 1–3). Thereafter, a Wilcoxon signed rank test in combination with a Bonferroni correction was applied to compare the visualization of each particular structure with both techniques (Table 4).

After the Bonferroni correction, a significant difference was found between SST and MSCT for the lateral malleolar ligament (Fig 4) and the bony septum between the upper and middle turn of the cochlea (Fig 5). The former was seen more clearly with MSCT, whereas the latter was seen better with SST.

Radiation Dose and Imaging Time

The average CTDI_{vol} was 50.3 mGy for MSCT and 16.8 mGy for SST. The average DLP was 306 mGy cm for MSCT and 64 mGy cm for SST.

Imaging time was 12.29 seconds for MSCT and 1 second for SST.

Discussion

High-resolution MR imaging and MSCT are the preferred tools for imaging the temporal bone. While high-resolution MR imaging has the advantage of excellent soft-tissue resolution, high-spatial-resolution MSCT is better at visualizing the delicate osseous structures and, thus, is the basis for the diagnosis of developmental anomalies, traumas, acute or chronic infections, and masses.^{1–4} Although the scanning time with modern MSCT scanners is short, especially in contrast to MR imaging, the patient must still remain motionless during the image acquisition, which can be a problem in uncooperative

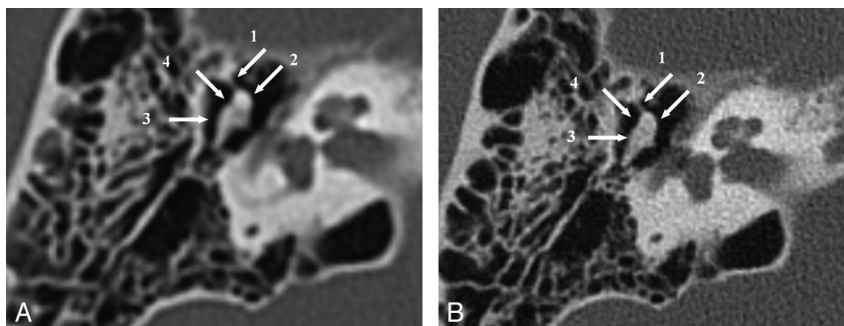


Fig 1. Temporal bone axial MPR, section thickness 0.8 mm, in both SST (A) and MSCT (B). The anterior malleal ligament (1), malleus head (2), incus body (3), and incudomalleal articulation (4) can be seen clearly with both imaging techniques.

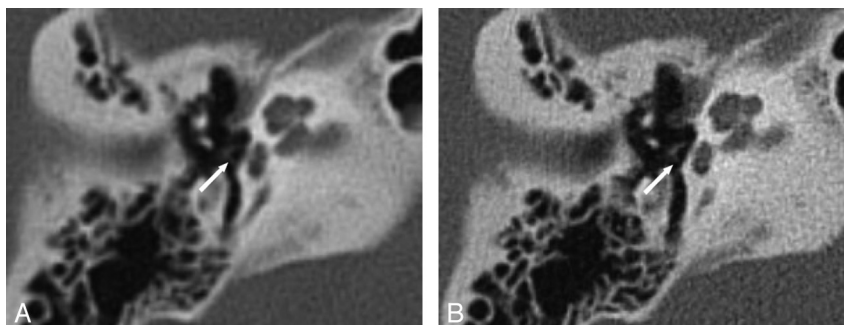


Fig 2. Temporal bone axial MPR, section thickness 0.8 mm, in both SST (A) and MSCT (B). The stapes crura (arrow) can be seen clearly with both imaging techniques.

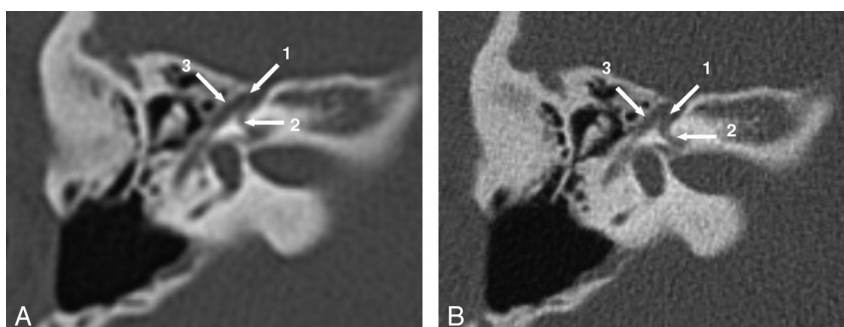


Fig 3. Facial nerve canal axial MPR, section thickness 0.8 mm, in both SST (A) and MSCT (B). The geniculate ganglion (1), labyrinthine segment (2), and the tympanic segment (3) of the facial nerve can be seen in diagnostic quality with both imaging techniques. Note the status postmastoidectomy.

patients or children. Another disadvantage of MSCT is that it exposes patients to rather high levels of ionizing radiation.

With the introduction of wider detector arrays, the SST (in which only 1 rotation of the tube-detector system is performed for data acquisition) became feasible for imaging whole-organ systems (eg, the heart or brain) or anatomic regions such as the temporal bone. The SST data in this study were acquired by using a 128-section MSCT system with a total volume coverage of 38.4 mm. Because the whole temporal bone is scanned with a single gantry rotation, imaging times of ≤ 1 second can be achieved. Therefore, even moderately cooperative patients could be examined with SST. Moreover, with our SST protocol, a dramatic decrease in radiation exposure could be achieved. As a negative effect, the higher section thickness of our SST resulted in an inferior resolution of the sections compared with MSCT, which was performed in the ultra-high-

resolution mode using a special grid in front of the detector array to reduce section thicknesses to 0.4 mm.

The aim of this study was to compare SST with MSCT to determine whether a compromise in the resolution of the SST would result in a reduced diagnostic value.

Although SST subjectively resulted in examinations that had less “sharp” images than MSCT using the ultra high resolution grid, the statistical comparison revealed no significant difference in the overall judgment of diagnostic image quality, whereas the separate evaluation showed a significant difference in 2 of 38 structures (5%).

The bony septum between the apical and middle turn of the cochlea could be judged significantly better with SST. The integrity of the latter together with, for example, the entire cochlear morphology is of special importance in the preoperative assessment of the inner ear before cochlear implanta-

Table 4: Difference between methods

Structure	P Value (Wilcoxon Signed Rank Test)	(a)	Alpha Value after Bonferroni Correction	(b)
Lateral malleal ligament	.000	x	.001	x
Bony septum between upper and middle turn of the cochlea	.000	x	.001	x
Round window membrane	.006	x	.001	
Vestibular aqueduct	.035	x	.001	
Stapedius muscle	.041	x	.001	
Stapes capitulum	.046	x	.002	
Stapes crura	.048	x	.001	
Cochlear aqueduct	.052		.002	
Anterior malleal ligament	.103		.002	
Anulus tympanicus	.131		.002	
Tendon of the musculus tensor tympani	.132		.002	
Superior malleal ligament	.145		.002	
Cochleariform process	.157		.002	
Crista falciformis	.157		.002	
Facial nerve canal: mastoid segment	.157		.002	
Tympanic membrane	.180		.002	
Malleus head	.317		.002	
Incus body	.317		.002	
Incus long process	.317		.002	
Incus short process	.317		.003	
Facial recess	.317		.003	
Facial nerve canal: tympanic segment	.317		.003	
Incudostapedial articulation	.320		.003	
Incus lenticular process	.371		.003	
Modiolus	.394		.004	
Scutum	1.000		.004	
Malleus handle	1.000		.004	
Incudomalleal articulation	1.000		.005	
Stapes footplate	1.000		.005	
Pyramidal eminence	1.000		.006	
Sinus tympani	1.000		.006	
Körner septum	1.000		.007	
Round window niche	1.000		.008	
Oval window	1.000		.01	
Ampulla membranaceum	1.000		.012	
Facial nerve canal: labyrinthine segment	1.000		.017	
Facial nerve canal: geniculate ganglion	1.000		.025	
Bony coverage of the facial nerve in the tympanic segment	1.000		.05	

(a) Significant after the Wilcoxon signed rank test.

(b) Significant after the Bonferroni correction.

tion⁸⁻¹⁰ or for the diagnosis of labyrinthitis ossificans.¹¹ Using SST could be an advantage in these patients.

The second anatomic structure that showed a significant difference between SST and MSCT was the lateral malleal ligament, which was imaged more clearly with MSCT. Because either fixation or detachment of the malleal ligaments may lead to impaired transduction of acoustic stimuli, a proper visualization of these delicate anatomic structures is necessary¹² and can be achieved with high-resolution CT.¹³ There-

fore, on the basis of our data, we recommend imaging of the malleal ligaments with MSCT rather than SST.

One major advantage of SST is its significantly shorter time of image acquisition. Our SST protocol took only 1 second compared with a duration of 12.29 seconds in our MSCT protocol. This decrease in imaging time of 92% could be of particular use in uncooperative persons and children, who sometimes have to undergo sedation or general anesthesia with all its drawbacks and risks.^{14,15} On the other hand, moving artifacts may theoretically lead to repetitive scans, which means additional radiation exposure.

The evaluation of our examinations showed no moving artifacts in the SST scans, whereas the image quality of MSCT was decreased due to patients' moving in 2 cases (Fig 6). Nevertheless, in both cases, image quality was sufficient to establish a diagnosis; thus, the examinations did not need to be repeated.

CT plays a major role in overall radiation exposure of patients. Therefore, it would be desirable to find radiation-saving techniques for CT. In this study, SST led to a reduction of the CTDI_{vol} and DLP of 67% and 79%, respectively, compared with MSCT with a comparable diagnostic quality and, thus, could be an interesting alternative.

A limitation of this study is that the highest possible spatial resolution of the MSCT protocol was not assessed. Whereas SST used a collimation of 0.75 mm, collimation was 0.4 mm with MSCT. However, image evaluation was performed with a constant section thickness of 0.8 mm for both SST and MSCT by using MPRs; thus, the 2 series were made comparable.

Moreover, a possible influence of the slightly different milliamperes-second (250 in SST versus 230 in MSCT) and FOV (200 in SST versus 141 in MSCT) on image quality requires discussion. Subsequent studies should be performed with image acquisition at constant section thicknesses, FOVs, and exposure parameters, to confirm our findings.

The evaluation was performed with a windowing of 4000 HU at a center of 700 HU; therefore, we do not think the contrast that was given for SST had any influence on the results of our study.

Because subjective image quality was different in SST and MSCT, a possible influence of this nonintended "unblinding" of the studies on the evaluation must be borne in mind. Although all examinations were performed to examine pathologies at the temporal bone, the visualization of these pathologies was not evaluated in this study. It is not clear whether using this new technique would be equally informative compared with MSCT in a specific disease process or patient population. This question has to be addressed in further investigations.

Conclusions

Our data show that SST and MSCT of the temporal bone do not differ significantly in terms of diagnostic quality if evaluated at a constant section thickness. In only 2/38 anatomic structures was a significant difference found, with MSCT being superior in 1 of those 2 instances. The shorter imaging time

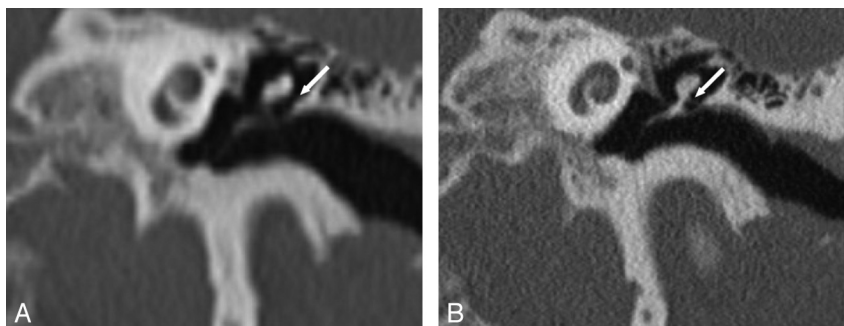


Fig 4. Temporal bone coronal MPR, section thickness 0.8 mm. The lateral malleolar ligament can hardly be seen with SST (A), whereas it is clearly shown with MSCT (B).

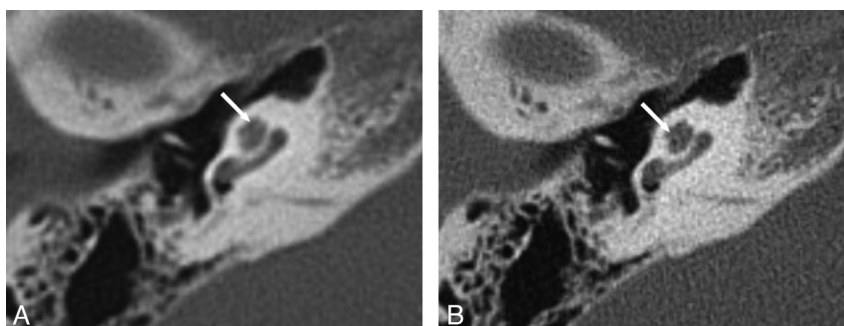


Fig 5. Temporal bone axial MPR, section thickness 0.8 mm. The bony septum between the apical and middle turn of the cochlea (arrows) can be seen more clearly with SST (A) than with MSCT (B), where it can hardly be found.



Fig 6. MSCT of the temporal bone, coronal (A) and axial (B) MPR, section thickness 0.8 mm. No moving artifacts are found in the SST scans, whereas the image quality of MSCT is decreased due to the patients moving in 2 cases (A and B). In 1 of those 2 individuals, the mastoid segment of the facial nerve canal (arrow) can barely be seen on the left side due to motion artifacts (B). However, image quality was sufficient to establish a diagnosis in both patients; thus, the examinations did not need to be repeated.

of SST may have particular application in uncooperative patients and children; in addition, all patients can benefit from the dramatic reduction of radiation exposure compared with MSCT.

References

1. Caldemeyer KS, Sandrasegaran K, Shinaver CN, et al. Temporal bone: comparison of isotropic helical CT and conventional direct axial and coronal CT. *AJR Am J Roentgenol* 1999;172:1675–82
2. Jager L, Bonell H, Liebl M, et al. CT of the normal temporal bone: comparison of multi- and single-detector row CT. *Radiology* 2005;235:133–41
3. Klingebiel R, Bauknecht HC, Rogalla P, et al. High-resolution petrous bone imaging using multi-slice computerized tomography. *Acta Otolaryngol* 2001;121:632–36
4. Lutz J, Jager V, Hempel MJ, et al. Delineation of temporal bone anatomy: feasibility of low-dose 64-row CT in regard to image quality. *Eur Radiol* 2007;17:2638–45
5. Hein PA, Romano VC, Lembcke A, et al. Initial experience with a chest pain protocol using 320-slice volume MDCT. *Eur Radiol* 2009;19:1148–55
6. Harnsberger H, Osborn A, Ross J, et al. *Diagnostic and Surgical Imaging Anatomy: Brain, Head and Neck, Spine*. Philadelphia: Lippincott Williams & Wilkins; 2006
7. Chuang MT, Chiang IC, Liu GC, et al. Multidetector row CT demonstration of inner and middle ear structures. *Clin Anat* 2006;19:337–44

8. Praetorius M, Staecker H, Plinkert PK. **Surgical technique in cochlear implantation** [in German]. *HNO* 2009;57:663–70
9. Westerhof JP, Rademaker J, Weber BP, et al. **Congenital malformations of the inner ear and the vestibulocochlear nerve in children with sensorineural hearing loss: evaluation with CT and MRI.** *J Comput Assist Tomogr* 2001;25:719–26
10. Colletti V, Fiorino FG, Carner M, et al. **Basal turn cochleostomy via the middle fossa route for cochlear implant insertion.** *Am J Otol* 1998;19:778–84
11. Karino S, Hayashi N, Aoki S, et al. **New method of using reconstructed images for assessment of patency of intracochlear spaces for cochlear implant candidates.** *Laryngoscope* 2004;114:1253–58
12. Dai C, Cheng T, Wood MW, et al. **Fixation and detachment of superior and anterior malleolar ligaments in human middle ear: experiment and modeling.** *Hear Res* 2007;230:24–33
13. Lemmerling MM, Stambuk HE, Mancuso AA, et al. **CT of the normal suspensory ligaments of the ossicles in the middle ear.** *AJNR Am J Neuroradiol* 1997;18:471–77
14. Kaste SC, Young CW, Holmes TP, et al. **Effect of helical CT on the frequency of sedation in pediatric patients.** *AJR Am J Roentgenol* 1997;168:1001–03
15. Malviya S, Voepel-Lewis T, Eldevik OP, et al. **Sedation and general anaesthesia in children undergoing MRI and CT: adverse events and outcomes.** *Br J Anaesth* 2000;84:743–48